# Posmom: The Unobserved Observable

Yves A. Bernard and Peter M. W. Gill*

Research School of Chemistry, Australian National University, Canberra ACT 0200, Australia

ABSTRACT We have recently shown that the probability density $S(s)$ of the position−momentum dot product $s = \mathbf{r} \cdot \mathbf{p}$ of a particle can be computed efficiently from its wave function $\psi(\mathbf{r})$. Here, by examining the H atom and LiH molecule, we show that $S(s)$ yields insight into the nature of electronic trajectories, and we argue that electron posmometry provides information that is inaccessible by diffraction or momentum methods.

SECTION Molecular Structure, Quantum Chemistry, General Theory
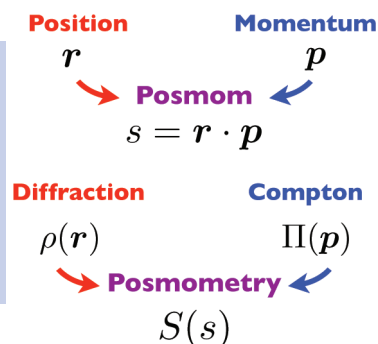
One of the first successful attempts to understand electronic behavior in matter was Bohr's famous model of the hydrogen atom.[1] By quantizing the angular momentum with an integer n (the principal quantum number), he sought to describe electronic motion using circular orbits, analogous to those of a planet. Some years later, Sommerfeld refined this model,[2] quantizing the z component of the angular momentum with another integer l to yield the Old Quantum Theory.[3] In this model, the electron follows elliptical orbits.

Although the Bohr−Sommerfeld (BS) model appeared to explain a number of features of atomic spectra, its insistence that electrons follow classical trajectories is essentially incorrect and has been superseded by modern quantum mechanical treatments. The advent of the Heisenberg Uncertainty Principle,[4] which states that the position $\mathbf{r}$ and the momentum $\mathbf{p}$ of a particle cannot be known simultaneously with arbitrary precision, showed that the classical concept of a trajectory begins to lose its significance in nanoscopic systems and must be abandoned completely in discussing the motion of an electron. In such circumstances, where classical mechanics aims to predict the position $\mathbf{r}$ of the particle at a time t, quantum mechanics more modestly (and correctly) offers only a wave function $\psi(\mathbf{r})$ which is related to the *probability* of finding the particle at the position $\mathbf{r}$ at time t.

In nonrelativistic wave mechanics,[5] the wave functions $\psi_n(\mathbf{r})$ and energies E_n of a particle are found by solving the Schrödinger equation $\mathbf{H}\psi_n = E_n\psi_n$ where $\mathbf{H}$ is the Hamiltonian operator for the system. As Dirac discovered,[6] these position wave functions are related to the particle's momentum wave functions $\phi_n(\mathbf{p})$ by a Fourier transform,[7] and this is depicted as a horizontal orange arrow in Figure 1. The fact that the product of the variance of a function and the variance of its Fourier transform is strictly positive is then the Schrödinger explanation for the Uncertainty Principle.

In the Born interpretation, the squared modulus of the wave function yields the corresponding probability density and, in this way, one can form the position density $\rho(\mathbf{r}) = |\psi(\mathbf{r})|^2$ and momentum density $\Pi(\mathbf{p}) = |\phi(\mathbf{p})|^2$ of the particle (Figure 1, blue arrows). Unlike the wave functions, the densities are experimental observables, and it is possible to measure $\rho(\mathbf{r})$ by X-ray[8] or neutron[9] diffraction and to measure $\Pi(\mathbf{p})$ by Compton spectroscopy.[10] Such techniques are widely used for the characterization of matter in condensed phases and furnish valuable information about molecular structure and bonding. We note that, although $\psi(\mathbf{r})$ and $\phi(\mathbf{p})$ contain the same information, the density $\rho(\mathbf{r})$ contains information that is not present in $\Pi(\mathbf{p})$, and vice versa.[11] In this way, position and momentum spectroscopy provide complementary perspectives.

The Fourier transforms in atomic units (the orange arrows at the top and bottom of Figure 1) of the position and momentum densities

$$\hat{\rho}(\mathbf{p}) = \int \rho(\mathbf{r})\mathrm{e}^{-i\mathbf{r}\cdot\mathbf{p}}\,\mathrm{d}\mathbf{r} \tag{1}$$

$$\hat{\Pi}(\mathbf{r}) = \int \Pi(\mathbf{p})\mathrm{e}^{-i\mathbf{r}\cdot\mathbf{p}}\,\mathrm{d}\mathbf{p} \tag{2}$$

are also important, and the convolution theorem shows[12] that $\hat{\Pi}(\mathbf{r})$ is the autocorrelation of the position wave function

$$\hat{\Pi}(\mathbf{r}) = \int \psi^*(\mathbf{r}' + \mathbf{r}/2)\psi(\mathbf{r}' - \mathbf{r}/2)\,\mathrm{d}\mathbf{r}' \tag{3}$$

and $\hat{\rho}(\mathbf{p})$ is the autocorrelation of the momentum wave function

$$\hat{\rho}(\mathbf{p}) = \int \phi^*(\mathbf{p}' + \mathbf{p}/2)\phi(\mathbf{p}' - \mathbf{p}/2)\,\mathrm{d}\mathbf{p}' \tag{4}$$

These connections are depicted by purple arrows in Figure 1. Thus, to compute the momentum density from the position wave function, one can take either the squared modulus of the Fourier transform, or the Fourier transform of the autocorrelation.
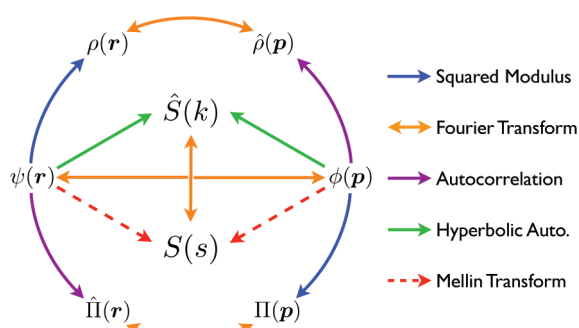
Figure 1. The relationships between the position, momentum, and posmom of a quantum mechanical particle.

A classical particle at $\mathbf{r}$ has a moment of inertia $I = mr^2$ about the origin. If the particle is moving, the rate at which I changes is $dI/dt = 2s$, where

$$s = \mathbf{r} \cdot \mathbf{p} \tag{5}$$

is the particle's *position*–*momentum* dot product, or posmom. The sum of the posmoms of all of the particles in a system is known as the virial.[13]

One may also consider the posmom of a quantum particle.[14,15] After symmetrizing eq 5, it can be shown that posmom is a quantum mechanical observable[16,17] and its wave function and density $S(s)$ are related nonbijectively[18] to the position and momentum wave functions by Mellin transforms[7] (the dashed red arrows in Figure 1). Unfortunately, the required transforms usually lead to formidable integrals and, until very recently, no such densities had been published.

However, we recently found[14] an alternative to the Mellin pathway by showing that the Fourier transform $\hat{S}(k)$ of the posmom density is given by the "hyperbolic autocorrelations"

$$\hat{S}(k) = \int \psi^*(e^{+k/2}\mathbf{r})\psi(e^{-k/2}\mathbf{r}) \, d\mathbf{r} \tag{6}$$

$$\hat{S}(k) = \int \phi^*(e^{-k/2}\mathbf{p})\phi(e^{+k/2}\mathbf{p}) \, d\mathbf{p} \tag{7}$$

of the position or momentum wave functions. Equations 6 and 7 (the green arrows in Figure 1) are analogous to the normal autocorrelations in eqs 3 and 4. After generating $\hat{S}(k)$, the inverse Fourier transform yields

$$S(s) = \frac{1}{2\pi} \int_{-\infty}^{\infty} \hat{S}(k)e^{iks} \, dk \tag{8}$$

(the vertical orange arrow in Figure 1) and, if necessary, this can be achieved by an efficient fast Fourier transform.[19] Time-reversal symmetry implies $S(s) = S(-s)$, so we can restrict our attention to $s \geq 0$.

Figure 1, which illustrates all of the interconnections between the position, momentum, and posmom wave functions and densities, is one of the important contributions of this letter.

The combination of eqs 6 and 8 enables the routine prediction of posmom densities in molecular systems using
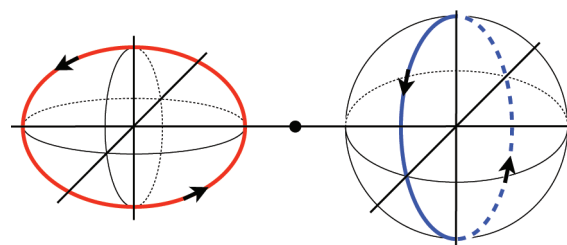

Figure 2. Two types of electron trajectory. The blue trajectory has $s = 0$, but the red trajectory yields a range of s values. The black dot marks an arbitrary origin along the horizontal axis.

standard methods of molecular physics. The definition eq 5 is origin-dependent so we choose the origins such that $\langle \mathbf{r} \rangle = \langle \mathbf{p} \rangle = 0$.

We have implemented this in a development version of the Q-CHEM quantum chemistry package[20] and, because of the low computational cost of eqs 6 and 8, the posmom densities of moderately large molecules can be computed on a desktop computer. For a 50-atom molecule with a triple-ζ-plus-polarization basis set, for example, the calculation of $\hat{S}(k)$ for a single value of k requires only a few seconds. We are currently investigating the posmom densities in atoms[21] and molecules.[22]

One may ask whether it feasible to find $S(s)$ from $\rho(\mathbf{r})$ and $\Pi(\mathbf{p})$, but this is extremely difficult.[11] Knowing nothing about the statistical correlation between $\mathbf{r}$ and $\mathbf{p}$, one is obliged to assume that they are independent and to write

$$S_{\text{indep}}(s) = \int \int \rho(\mathbf{r})\Pi(\mathbf{p})\delta(s - \mathbf{r} \cdot \mathbf{p}) \, d\mathbf{r} \, d\mathbf{p} \tag{9}$$

and this is completely different from the true $S(s)$ given by eq 8. For a harmonic oscillator, for example, one finds[14]

$$S(s) = (2\pi)^{-3/2} \left| \Gamma\left(\frac{1}{4} + \frac{is}{2}\right) \right|^2 \tag{10}$$

$$S_{\text{indep}}(s) = (2/\pi)K_0(2s) \tag{11}$$

where Γ and K_0 are Gamma and modified Bessel functions.[23]

We conclude that the posmom density contains information that is inaccessible from position or momentum spectroscopies. But how can its measurement give insight into electronic motion? If a particle moves in a circular (or cylindrical) orbit that preserves its distance from the origin (e.g., the blue curve in Figure 2), its position and momentum are orthogonal at all times, its posmom vanishes, and its posmom density $S(s)$ is a delta function at $s = 0$. In contrast, if the particle follows a highly eccentric Keplerian ellipse (e.g., the red curve in Figure 2), its position and momentum are almost parallel (or antiparallel), its posmom swings between positive and negative values, and $S(s)$ is broad.

Thus, given the posmom density in an electronic system, one can deduce something about the types of trajectories that the electrons follow. To illustrate this, we will examine the posmom distributions in various states of the hydrogen atom and the lithium hydride molecule.
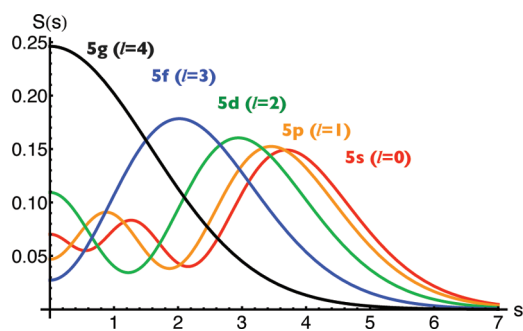
Figure 3. Posmom densities of the $n = 5$ states of the hydrogen atom.

The posmom density for the (n,l,m) state of the H atom can be found, using eqs 6 and 8, from the position wave function

$$\psi(\mathbf{r}) = \sqrt{\left(\frac{2}{n}\right)^3 \frac{(n-l-1)!}{2n(n+l)!}}\, e^{-r/n}(2r/n)^l L_{n-l-1}^{2l+1}(2r/n)Y_{lm}(\mathbf{r}) \quad (12)$$

where L_{n-l-1}^{2l+1} is an associated Laguerre polynomial, and Y_{lm} is a spherical harmonic. This yields

$$S(s) = \frac{(-1)^{n-l-1}(n+l)!}{(n-l-1)!(2l+1)!} \frac{\left|\Gamma\left(l+\frac{3}{2}+is\right)\right|^2}{\Gamma\left(\frac{1}{2}\right)\Gamma\left(l+\frac{3}{2}\right)\Gamma(l+2)}$$

$$\times\, {}_4F_3\left[\begin{array}{cccc} -(n-l-1) & n+l+1 & l+\frac{3}{2}+is & l+\frac{3}{2}-is \\ l+\frac{3}{2} & l+2 & 2l+2 \end{array}\right] \quad (13)$$

(where ${}_4F_3$ is a generalized hypergeometric function[24]), which is independent of the quantum number m. It can be shown that the variance of $S(s)$ is

$$\sigma^2 = \frac{n^2}{2} - \frac{l(l+1)}{2} + \frac{1}{4} \quad (14)$$

and this decreases monotonically as l increases for a fixed n. The density at $s = 0$ is

$$S(0) = \frac{1}{n\pi}\left[\frac{\Gamma\left(\frac{n-l+1}{2}\right)\Gamma\left(\frac{n+l+1}{2}\right)}{\Gamma\left(\frac{n-l}{2}\right)\Gamma\left(\frac{n+l+2}{2}\right)}\right]^{\beta} \quad (15)$$

where $\beta = (-1)^{n-l}$. This oscillates as l increases, creating an increasing subsequence for odd $n-l$ and a decreasing subsequence for even $n-l$. As a result, the largest $S(0)$ occurs for $l = n-1$ and the smallest $S(0)$ occurs for $l = n-2$.

It can be shown that, when n is large and $l = n-1$, the density $S(s)$ approaches a Normal distribution.

Figure 3 depicts the densities for the states with $n = 5$, and Table 1 contains associated numerical data. Radial nodes in $\psi(\mathbf{r})$ create oscillations in $S(s)$, and the posmom densities extend significantly into the nonclassical region beyond their final points of inflection s_{inf}. The most probable posmom values

Table 1. Variance, Origin Density, and Classical Turning Points of the Posmom Density in the $n = 5$ States of the Hydrogen Atom

	exact			semiclassical		
	σ^2	$S(0)$	s_{inf}	σ_{EBK}^2	$S_{\text{EBK}}(0)$	s_{max}
5s	12.75	0.070	4.64	19.5	0.001	4.97
5p	11.75	0.047	4.42	17.2	0.008	4.77
5d	9.75	0.109	3.95	13.2	0.022	4.33
5f	6.75	0.027	3.14	8.15	0.047	3.57
5g	2.75	0.246	1.56	2.68	0.114	2.18

in the 5s state are near $s \pm 4$, but the variance decreases with l, and the most probable value in the (almost normally distributed) 5g state is $s = 0$. In the trajectory interpretation, this shows that 5s electrons rarely follow circular paths, but that 5g electrons may do so much more often.

It is interesting to compare these results with a semiclassical approximation. The Einstein−Brillouin−Keller (EBK) model[25] applied to the hydrogen atom[26,27] is similar to the BS model, yielding elliptical orbits with semimajor axes, semiminor axes, and eccentricities given by

$$a = n^2 \quad (16)$$

$$b = n(l+1/2) \quad (17)$$

$$\varepsilon = \sqrt{1 - b^2/a^2} \quad (18)$$

The density given by the EBK model is

$$S_{\text{EBK}}(s) = \frac{1}{\pi - 2\varepsilon}\left(\frac{1}{\sqrt{s_{\text{max}}^2 - s^2}} - \frac{1}{n}\right) \quad |s| < s_{\text{max}} \quad (19)$$

where $s_{\text{max}} = n\varepsilon$. Unlike the exact density, this grows monotonically with $|s|$. The variance of $S_{\text{EBK}}(s)$ is

$$\sigma_{\text{EBK}}^2 = \frac{s_{\text{max}}^2}{2}\left(1 + \frac{2}{3}\frac{\varepsilon}{\pi - 2\varepsilon}\right) \quad (20)$$

which decreases monotonically as l increases. However, in the limit of large n and l, the semiclassical and exact models converge (as required by the Correspondence Principle) and predict

$$\sigma^2 \sim n/2 \quad (21)$$

The density at $s = 0$ is

$$S_{\text{EBK}}(0) = \frac{1 - \varepsilon}{n\varepsilon(\pi - 2\varepsilon)} \quad (22)$$

which increases monotonically from $S_{\text{EBK}}(0) = O(n^{-3})$ at $l = 0$ to $S_{\text{EBK}}(0) = O(n^{-1/2})$ at $l = n - 1$.

Figure 4 shows the EBK trajectories for the $n = 5$ states, and Table 1 contains associated numerical data. As l increases, the trajectory shifts from a highly elliptical path in the 5s state to an almost circular orbit in the 5g state. However, the EBK model usually overestimates the variance.

The data in Table 1 confirm that, although a semiclassical treatment captures some of its features, the exact description of the posmom density is significantly richer and more detailed.
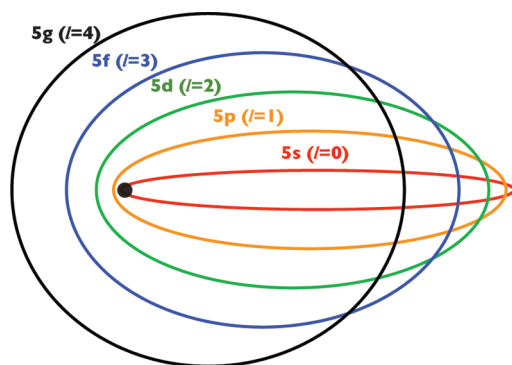
Figure 4. Semiclassical (EBK) orbits of the $n = 5$ states of the hydrogen atom. The black dot shows the proton, which was used as the origin for **r**.
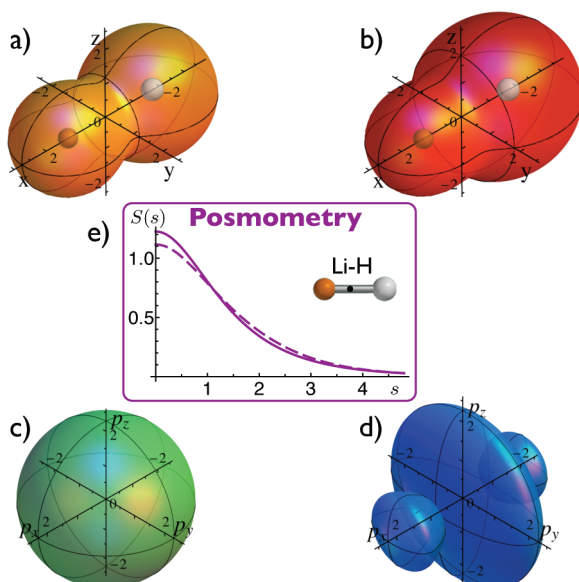

Figure 5. Position, momentum and posmom densities in the LiH protomolecule and molecule ($R = 3$ au) centered at $\langle \mathbf{r} \rangle = \langle \mathbf{p} \rangle = 0$, based on HF/6-311G(3df,3pd) wave functions. (a) $\rho(\mathbf{r})$ in the protomolecule; (b) $\rho(\mathbf{r})$ in the molecule; (c) $\Pi(\mathbf{p})$ in the protomolecule; (d) $\Pi(\mathbf{p})$ in the molecule; (e) $S(s)$ in the protomolecule (dashed) and in the molecule (solid). Diagrams a—d depict 0.01 iso-surfaces.

We now turn from a simple atom to a simple molecule. What new insight, inaccessible from the position and momentum densities, can be gained from $S(s)$? Figure 5 shows various densities in the LiH molecule, both before and after bond formation.

Diagrams a and b, which show the position densities, reveal that bond formation is associated with significant shift of charge density from the Li atom to the H atom, as one would have anticipated from the electronegativities of these atoms.

Diagrams c and d, which show the momentum densities, indicate that the previously isotropic distribution of momentum becomes strongly anisotropic and develops nodal surfaces near $p_x = \pm 1$ when the bond forms.

Diagram e reveals that the posmom density narrows during bond formation, the density at $s = 0$ increasing by

roughly 10 %. In the trajectory interpretation, this implies that bond formation encourages the electrons to forsake motion *parallel* or *perpendicular* to the molecular axis in favor of paths *around* it. Although this picture is consistent with the momentum density in diagram d, it cannot be deduced from it.

There is no doubt that $\rho(\mathbf{r})$ and $\Pi(\mathbf{p})$ help us to comprehend the electronic structure of molecules, but it is equally clear that $S(s)$ offers additional insight. The three densities are mutually complementary.

This letter aims to draw attention to posmom, a basic quantum mechanical observable that has been largely overlooked. The relationships between posmom, position, and momentum are summarized in Figure 1. Recent progress now allows the posmom density $S(s)$ to be calculated routinely from the position wave function $\psi(\mathbf{r})$, and we have implemented this in a development version of the Q-CHEM software package.

In a comprehensive study of the states of the hydrogen atom, we have found that semiclassical approximations fail to reproduce the detailed structure of $S(s)$ and are an inadequate substitute for it. An examination of $S(s)$ in the LiH molecule confirmed that it contains information about electronic motion that is absent from the position or momentum densities. Whereas diffraction techniques reveal where electrons *are*, and momentum spectroscopy tells us where they are *going*, posmometry (the measurement of posmom) informs us—without violating the Uncertainty Principle—about the *type of trajectories* that they follow. Potentially, this third perspective can significantly enrich our appreciation of the dynamical behavior of electrons.

We eagerly await the construction of the first posmometers.

AUTHOR INFORMATION

Corresponding Author:
*To whom correspondence should be addressed. E-mail: peter.gill@anu.edu.au.

REFERENCES

(1) Bohr, N. On the Constitution of Atoms and Molecules. *Philos. Mag.* **1913**, *26*, 1–24.

(2) Sommerfeld, A. *Atombau und Spektrallinien*; Friedrich Vieweg und Sohn: Braunschweig, 1919.

(3) ter Haar, D. *The Old Quantum Theory*; Pergamon Press: Oxford, 1967.

(4) Heisenberg, W. Uber den Anschaulichen Inhalt der Quantentheoretischen Kinematik und Mechanik. *Z. Phys.* **1927**, *43*, 172–198.

(5) Schrödinger, E. Quantisierung als Eigenwertproblem. *Ann. Phys.* **1926**, *79*, 361–376.

(6) Dirac, P. A. M. *The Principles of Quantum Mechanics*; Clarendon Press: Oxford, 1958.

(7)   Debnath, L.; Bhatta, D. *Integral Transforms and Their Applications*; Chapman & Hall: Boca Raton, FL, 2007.

(8)   Sands, D. E. *Introduction to Crystallography*; Benjamin: New York, 1969.

(9)   Wilson, C. C. *Single Crystal Neutron Diffraction from Molecular Materials*; World Scientific: Singapore, 2000.

(10)   Weigold, E.; McCarthy, I. E. *Electron Momentum Spectroscopy*; Kluwer: New York, 1999.

(11)   Via a Hohenberg–Kohn argument, it is possible *in principle* to obtain $\Pi(\mathbf{p})$ from $\rho(\mathbf{r})$, but *in practice* this is almost impossible.

(12)   Benesch, R.; Singh, S. R.; Smith, V. H., Jr. On the Relationship of the X-Ray form Factor to the 1-Matrix in Momentum Space. *Chem. Phys. Lett.* **1971**, *10*, 151–153.

(13)   Goldstein, H. *Classical Mechanics*, 2nd ed.; Addison-Wesley: Cambridge, MA, 1980.

(14)   Bernard, Y. A.; Gill, P. M. W. The Distribution of $\mathbf{r} \cdot \mathbf{p}$ in Quantum Mechanical Systems. *New J. Phys.* **2009**, *11*, 083015 (15 pp).

(15)   Twamley, J.; Milburn, G. J. The Quantum Mellin Transform. *New J. Phys.* **2006**, *8*, 328 (20 pp).

(16)   Wess, J. The Conformal Invariance in Quantum Field Theory. *Il Nuovo Cimento* **1960**, *18*, 1086–1107.

(17)   The reader may be interested in the conjugate variable of the posmom *s*. In the position representation, it is given by $\ln(r)$; see ref 15.

(18)   Itzykson, C. Group Representation in a Continous Basis - An Example. *J. Math. Phys.* **1969**, *10*, 1109–1114.

(19)   van Loan, C. *Computational Frameworks for the Fast Fourier Transform*; SIAM: Philadelphia, 1987.

(20)   Shao, Y.; et al. Advances in Methods and Algorithms in a Modern Quantum Chemistry Program Package. *Phys. Chem. Chem. Phys.* **2006,** *8*, 3172–3191.

(21)   Bernard, Y. A.; Crittenden, D. L.; Gill, P. M. W. Posmom Densities in Atomic Systems. Manuscript in preparation.

(22)   Bernard, Y. A.; Crittenden, D. L.; Gill, P. M. W. Posmom Densities in Molecular Systems. Manuscript in preparation.

(23)   Abramowitz, M.; Stegun, I. E. *Handbook of Mathematical Functions*; Dover: New York, 1972.

(24)   Slater, L. J. *Generalized Hypergeometric Functions*; Cambridge University Press: Cambridge, England, 2008.

(25)   Keller, J. B. Corrected Bohr–Sommerfeld Quantum Conditions for Nonseparable Systems. *Ann. Phys.* **1958,** *4*, 180–188.

(26)   Curtis, L. J.; Ellis, D. G. Use of the Einstein–Brillouin–Keller Action Quantization. *Am. J. Phys.* **2004,** *72*, 1521.

(27)   Curtis, L. J.; Ellis, D. G. Probabilities as a Bridge Between Classical and Quantum-Mechanical Treatments. *Eur. J. Phys.* **2006,** *27*, 485–496.